

RD-A162 944

NUCLEAR WEAPON EFFECT RESEARCH AT PSR (PACIFIC-SIERRA
RESEARCH CORPORATION. (U) PACIFIC-SIERRA RESEARCH CORP
LOS ANGELES CA L SCHLESSINGER 28 SEP 84 PSR-1422-VOL-8
DNA-TR-84-308-V8 DNA#01-83-C-0015

1/1

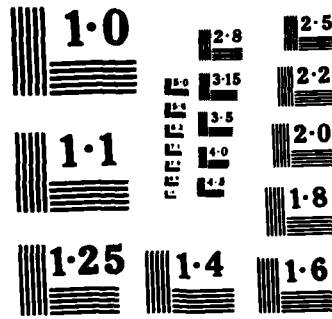
UNCLASSIFIED

F/G 18/3

ML

END

PIMED
--
DTIC



NATIONAL BUREAU OF STANDARDS
MICROCOPY RESOLUTION TEST CHART

6

E 301868

DNA-TR-84-308-V8

AD-A162 944

NUCLEAR WEAPON EFFECT RESEARCH AT PSR—1983
Volume VIII—Effect of Shock-Induced Ground Conductivity on Kratz
Particle Velocity Gauge

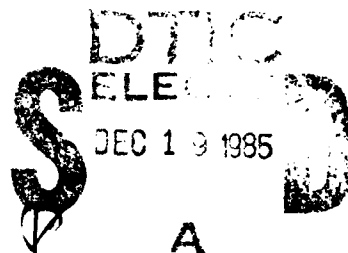
Leonard Schlessinger
Pacific-Sierra Research Corporation
12340 Santa Monica Boulevard
Los Angeles, CA 90025-2587

28 September 1984

Technical Report

CONTRACT No. DNA 001-83-C-0015

Approved for public release;
distribution is unlimited.



THIS WORK WAS SPONSORED BY THE DEFENSE NUCLEAR AGENCY
UNDER RDT&E RMSS CODE B350083466 P99QAXDB00200 H2590D.

ONE COPY
ONE COPY

Prepared for
Director
DEFENSE NUCLEAR AGENCY
Washington, DC 20305-1000

Destroy this report when it is no longer needed. Do not return
to sender.

PLEASE NOTIFY THE DEFENSE NUCLEAR AGENCY,
ATTN: STTI, WASHINGTON, DC 20305-1000, IF YOUR
ADDRESS IS INCORRECT, IF YOU WISH IT DELETED
FROM THE DISTRIBUTION LIST, OR IF THE ADDRESSEE
IS NO LONGER EMPLOYED BY YOUR ORGANIZATION.



UNCLASSIFIED

SECURITY CLASSIFICATION OF THIS PAGE

AD-A162 944

Form Approved
OMB No. 0704-0188
Exp. Date: Jun 30, 1986

REPORT DOCUMENTATION PAGE			
1a. REPORT SECURITY CLASSIFICATION UNCLASSIFIED		1b. RESTRICTIVE MARKINGS	
2a. SECURITY CLASSIFICATION AUTHORITY		3. DISTRIBUTION/AVAILABILITY OF REPORT Approved for public release; distribution is unlimited.	
2b. DECLASSIFICATION/DOWNGRADING SCHEDULE N/A since UNCLASSIFIED		5. MONITORING ORGANIZATION REPORT NUMBER(S) DNA-TR-84-308-V8	
4. PERFORMING ORGANIZATION REPORT NUMBER(S) PSR Report 1422		7a. NAME OF MONITORING ORGANIZATION Director Defense Nuclear Agency	
6a. NAME OF PERFORMING ORGANIZATION Pacific-Sierra Research Corporation	6b. OFFICE SYMBOL (if applicable)	7b. ADDRESS (City, State, and ZIP Code) Washington, DC 20305-1000	
6c. ADDRESS (City, State, and ZIP Code) 12340 Santa Monica Boulevard Los Angeles, CA 90025-2587		9. PROCUREMENT INSTRUMENT IDENTIFICATION NUMBER DNA 001-83-C-0015	
8a. NAME OF FUNDING/SPONSORING ORGANIZATION		8b. OFFICE SYMBOL (if applicable)	
8c. ADDRESS (City, State, and ZIP Code)		10. SOURCE OF FUNDING NUMBERS	
		PROGRAM ELEMENT NO. 62715H	PROJECT NO. P99QAXD
		TASK NO. B	WORK UNIT ACCESSION NO. DH006427
11. TITLE (Include Security Classification) NUCLEAR WEAPON EFFECT RESEARCH AT PSR—1983 Volume VIII—Effect of Shock-Induced Ground Conductivity on Kratz Particle Velocity Gauge			
12. PERSONAL AUTHOR(S) Leonard Schlessinger			
13a. TYPE OF REPORT Technical	13b. TIME COVERED FROM <u>821027</u> TO <u>821130</u>	14. DATE OF REPORT (Year, Month, Day) 1984, September 28	15. PAGE COUNT 38
16. SUPPLEMENTARY NOTATION This work was sponsored by the Defense Nuclear Agency under RDT&E RMSS Code B350083466 P99QAXDB00200 H2590D.			
17. COSATI CODES		18. SUBJECT TERMS (Continue on reverse if necessary and identify by block number)	
FIELD 18	GROUP 3	Particle Velocity Gauge Underground Test Cratering	Ground Motion Nuclear Test Instrumentation MINI JADE
19	4		
19. ABSTRACT (Continue on reverse if necessary and identify by block number)			
<p>This report details the effect of shock-induced conductivity on the operation of the Kratz velocity gauge, which measures the ground particle velocity induced by the shock wave due to a large-yield high-explosive or underground nuclear detonation. Such shock waves are typically strong enough to induce significant ground conductivity, which can affect the operation of the gauge. Three models of increasing fidelity to the physics of the advancing conductivity front are presented and analyzed. Numerical results indicate that, for typical gauge parameter values, shock-induced ground conductivities of 100 mhos/m or less do not affect gauge response.</p>			
20. DISTRIBUTION/AVAILABILITY OF ABSTRACT <input type="checkbox"/> UNCLASSIFIED/UNLIMITED <input checked="" type="checkbox"/> SAME AS RPT <input type="checkbox"/> DTIC USERS		21. ABSTRACT SECURITY CLASSIFICATION UNCLASSIFIED	
22a. NAME OF RESPONSIBLE INDIVIDUAL Betty L. Fox		22b. TELEPHONE (Include Area Code) (202) 325-7042	22c. OFFICE SYMBOL DNA/STTI

SUMMARY

This report details the effect of shock-induced conductivity on the operation of the Kratz velocity gauge, which measures the ground particle velocity induced by the shock wave due to a large-yield high-explosive or underground nuclear detonation. The Kratz gauge operates by sensing the time rate of change of the magnetic field produced by a field coil embedded in and ideally moving with the medium. The shock wave from a large-yield detonation can induce significant conductivity in the ground, which can in turn affect gauge response both before and after the shock wave passes the field coil.

Three models of increasing fidelity to the physics of the advancing conductivity front are presented and analyzed, the third being the most complex and most accurate. Numerical results presented for model 3 indicate that, for typical gauge parameter values, shock-induced ground conductivities of 100 mhos/m or less do not affect gauge response.



A/

PREFACE

This report is one of a multivolume set comprising the Pacific-Sierra Research Corporation (PSR) final report on Defense Nuclear Agency (DNA) contract DNA001-83-C-0015. The work done under this contract spans a wide range of nuclear weapon effect research covering airblast, cratering and ground motion, intermediate-dose radiation, underground test design and development, fire research, and electromagnetic pulse research.

This volume details the effect of shock-induced conductivity on the operation of the Kratz particle velocity gauge. The project officer was Michael J. Frankel, and the technical monitor was David L. Auton.

TABLE OF CONTENTS

<u>Section</u>		<u>Page</u>
SUMMARY		1
PREFACE		2
1 INTRODUCTION		5
2 KRATZ GAUGE OPERATION AND THREE MODELS		6
3 ANALYSIS OF MODELS 1 AND 2		9
Derivation of basic equations		9
Green's function		10
Evaluation of voltage in pickup coil		13
4 ANALYSIS OF MODEL 3		15
5 NUMERICAL RESULTS		23
REFERENCES		27
APPENDIX		
LIST OF SYMBOLS		29

SECTION 1
INTRODUCTION

The Kratz particle velocity gauge [Kratz, 1976] is designed to measure the particle velocity in the ground induced by a shock wave due to chemical or nuclear explosives. It has been successfully used in several high-explosive tests as well as the nuclear underground tests (UGTs) HURON LANDING and MINI JADE. It is to be deployed on several other UGTs, including MISTY JADE. The Kratz gauge is typically used to measure velocities ranging from 3×10^3 m/sec (peak) to 8×10^2 m/sec (peak), decaying with a time constant of 10 to 100 μ sec. The period over which measurements are made is a few time constants.

Both Kratz [1976] and Schlessinger [1981] presented and evaluated the basic theory for calibrating the gauge and quantifying its operation, but neither completely modeled the electrical conductivity induced in the medium by the advancing shock wave. Schlessinger demonstrated, though only approximately, that the shock-induced conductivity would not significantly influence the gauge response for a wide range of relevant gauge parameter values. However, the high quality of data recently obtained from the gauge [Coleman, 1982, 1983] may permit us to identify and quantify even the small changes in gauge response caused by the shock-induced conductivity. A better theory to describe those small signals could explain the data more thoroughly.

This report details the effect of shock-induced conductivity on Kratz gauge operation. Because the problem is so complex, we present and analyze three models of increasing fidelity to the physics of the moving conductivity front, the third being the most complex and most accurate. For model 3, we give numerical results that can be used to quantify the effect of the shock-induced ground conductivity.

SECTION 2

KRATZ GAUGE OPERATION AND THREE MODELS

Detailed descriptions of the gauge and its operation are given by Kratz [1976] and Coleman [1982]. Basically, the gauge consists of a field coil and several pickup coils. The field coil comprises several turns of wire embedded in an aluminum disk. Current is run through the coil. At the time of the explosion, the external current is turned off but, because the coil is in aluminum, current persists for a time long compared with the measurement times of interest. Thus, the current in the field coil can be considered constant in time. The shock wave approaches and overtakes the field coil as shown in Fig. 1. After the shock wave passes, the field coil ideally should move with the particle velocity of the medium. A voltage proportional to the rate of change of the magnetic field and related to the field coil velocity is induced in the pickup coils, located some distance from the field coil.

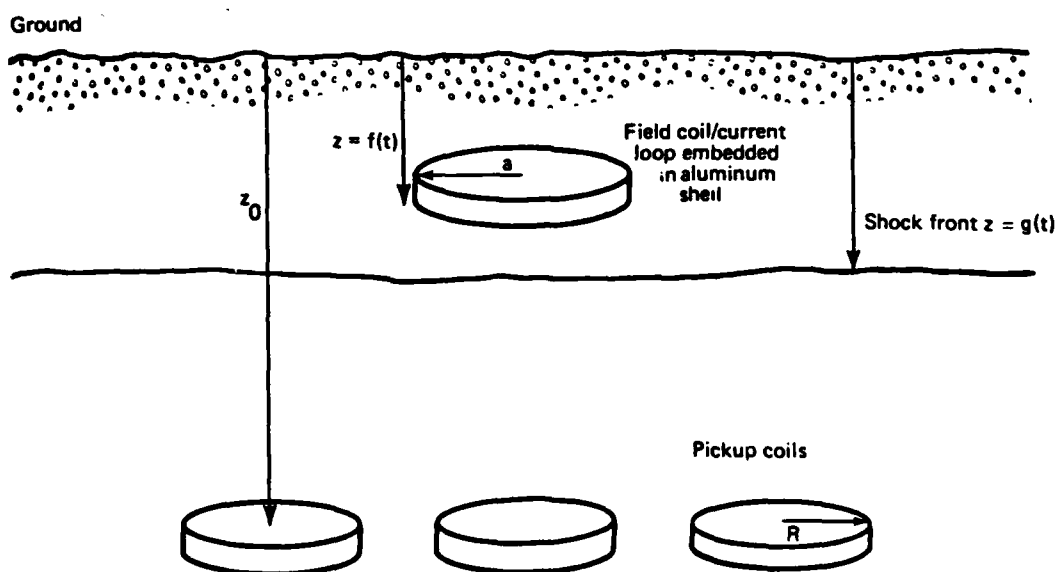


Figure 1. Gauge geometry.

The relationship between the field coil velocity and the voltage in the pickup coil is modified by the ambient and shock-induced conductivities of the intervening medium. The ambient conductivity allows eddy currents induced by the changing magnetic field of the field coil to flow in the medium. The currents produce magnetic field changes that tend to cancel those produced by the moving field coil. If the cancellation is significant, the signal recorded by the pickup coil will be badly distorted.

The shock-induced conductivity can have two effects. First, the pickup coil responds to the changing magnetic field produced by the advancing conductivity front even before the shock wave arrives at the field coil. Second, the shock-induced conductivity can modify the gauge response after the shock wave passes the field coil. The shock wave produces conductivity between the field coil and the pickup coil, thus modifying the response as described above by allowing even greater eddy currents in the medium.

We have developed three models to describe those effects. The models differ only in their treatment of the moving conductivity front; they share the same description of the field and pickup coils. The field coil is taken to be a current loop of radius a centered at $z = 0$, $r = 0$ of a cylindrical coordinate system. The field coil carries a constant current I and moves in the z direction with velocity $v(t)$ at time t . The position of the field coil is given by

$$f(t) = \int_{-\infty}^t v(t') dt' .$$

The pickup coil is a single loop of radius R centered at $z = z_0$, $r = 0$ in the z , r plane

Model 1 assumes that the coils are embedded in a medium of constant conductivity σ and that the medium is moving with a constant velocity v_0 in the coordinate system stationary with respect to the pickup coil. The results of model 1 were presented previously [Schlessinger, 1981] and are only summarized here. The model demonstrated that the effects of the ambient conductivity were negligible for all parameter values of interest

and that the shock-induced conductivity was not crucial (for typical values) until it reached about 100 mhos/m.

Model 2 resembles model 1 but more completely describes the moving conductivity front. It assumes that the medium velocity is a function of time-- $v_0(t)$. Both models assume that the medium conductivity extends throughout all space and is constant in space, and that the entire medium is moving with respect to the pickup coil. The results of model 2 are the same as those of model 1 when v_0 is held constant. Model 2 shows that when $v_0(t)$ is equal to $v(t)$ --that is, when the field coil velocity and the medium velocity are the same--the medium conductivity has no effect. Further, when there are small differences in $v_0(t)$ and $v(t)$, the medium conductivity begins to have a noticeable effect, for typical gauge parameter values, when it reaches 100 mhos/m.

Model 3 was devised to overcome the deficiencies in models 1 and 2 and to be used for quantifying the small but perhaps noticeable effects of shock conductivity. In model 3, the medium conductivity and velocity are allowed to change as functions of space and time. The medium has conductivity σ for positions $z < g(t)$ and conductivity 0 for positions $z > g(t)$, where the function $g(t)$ represents the position of the shock wave. The medium is moving with velocity $v_0(t)$ for $z < g(t)$ and is at rest for $z > g(t)$. This model describes the physics of the moving conductivity front much more accurately, but is considerably more difficult to describe and analyze mathematically.

SECTION 3

ANALYSIS OF MODELS 1 AND 2

Models 1 and 2 are so similar that they can be analyzed together. The only difference between them is that the medium velocity $v_0(t)$ is a constant for model 1 but can vary over time for model 2. The major steps in the analysis are as follows. First, we derive the equations of the vector potential \vec{A} generated by the current density \vec{J} in the field coil. Second, the equations for \vec{A} are solved by finding their Green's function. Third, we evaluate the voltage in the pickup coil generated by the vector potential \vec{A} . We use mks units throughout this report.

DERIVATION OF BASIC EQUATIONS

The Maxwell equations for the electric field \vec{E} and the magnetic field \vec{B} in a medium of conductivity σ moving with velocity $v_0(t)$ are

$$\vec{\nabla} \times \vec{E} = - \frac{\partial \vec{B}}{\partial t} \quad (1)$$

and

$$\vec{\nabla} \times \vec{B} = \mu [\vec{J} + \sigma (\vec{E} + \vec{v}_0 \times \vec{B})] , \quad (2)$$

where μ is the medium permeability. In our case, the current density \vec{J} of the field coil has a component only in the ϕ direction of a cylindrical coordinate system and is given by

$$J = I\delta(r - a)\delta(z - f(t)) , \quad (3)$$

where I is the constant current, $\delta(x)$ is the Dirac delta function, r and z are the radial and axial coordinates, respectively, of the cylindrical coordinate system, a is the radius of the field coil, and $f(t)$ gives the position of the field coil at time t .

To solve Eqs. (1) and (2), we introduce the vector potential \vec{A} , satisfying

$$\vec{B} = \vec{\nabla} \times \vec{A} .$$

It follows from Eq. (1) that

$$\vec{E} = - \vec{\nabla} \phi - \frac{\partial \vec{A}}{\partial t} ,$$

where Φ is the scalar potential. We choose the gauge such that

$$\vec{\nabla} \cdot \vec{A} + \mu\sigma\phi = 0 .$$

Because the current flows only in the ϕ direction, \vec{A} has only a ϕ component that satisfies

$$\nabla^2 A - \frac{A}{r^2} - \mu\sigma \frac{\partial A}{\partial t} - \mu\sigma v_0(t) \frac{\partial A}{\partial z} = - \mu J . \quad (4)$$

Here we have assumed that the velocity $v_0(t)$ has a component only in the z direction. Equation (4) must be solved for A , which can then be used to find the voltage in the field coil.

GREEN'S FUNCTION

A standard method of solving an equation like Eq. (4) is to find its Green's function G . For Eq. (4), that is the solution of

$$\left(\nabla^2 - \frac{1}{r^2} - \mu\sigma \frac{\partial}{\partial t} - \mu\sigma v_0 \frac{\partial}{\partial z} \right) G(r, r', z, z', t, t') \\ = \delta(r - r')\delta(z - z')\delta(t - t') . \quad (5)$$

Given the Green's function, the solution to Eq. (4) is

$$A(r, z, t) = -\mu \int dr' dz' dt' G(r, r', z, z', t, t') J(r', z', t') . \quad (6)$$

To find G , we express the delta function in a Fourier-Bessel representation:

$$\delta(r - r')\delta(z - z') = \frac{1}{2\pi} \iint dk d\xi e^{ik(z-z')} \xi J_1(\xi r) J_1(\xi r') , \quad (7)$$

where $J_1(x)$ is a first-order Bessel function. We also express G in the same form as

$$G(r, r', z, z', t, t') = \frac{1}{2\pi} \iint dk d\xi e^{ik(z-z')} \times \xi J_1(\xi r) J_1(\xi r') \hat{G}(k, \xi, t) . \quad (8)$$

The equation for \hat{G} follows from Eqs. (5), (7), and (8):

$$(k^2 + \xi^2)\hat{G}(k, \xi, t) + i\mu\sigma kv_0 \hat{G} + \mu\sigma \frac{\partial \hat{G}}{\partial t} = -\delta(t - t') . \quad (9)$$

Equation (9) can be solved to obtain

$$\hat{G}(k, \xi, t) = -\frac{\theta(t - t')}{\mu\sigma} \exp - \int_{t'}^t \left\{ \left[\frac{k^2 + \xi^2}{\sigma} + ikv_0(t'') \right] dt'' \right\} , \quad (10)$$

where

$$\theta(x) = 1 , \quad x > 0 ,$$

$$\theta(x) = 0 , \quad x < 0 .$$

Thus, the Green's function can be written in integral form using Eqs. (8) and (10), which can be further reduced by performing some of the

integrations. The ξ integration can be performed using the result [Gradsteyn and Ryzhik, 1980]

$$\int_0^\infty \xi J_1(\xi r) J_1(\xi r') \exp -\frac{\xi^2}{\mu\sigma} (t - t') = \frac{\mu\sigma}{2(t - t')} \exp \left[-\frac{(r^2 + r'^2)\mu\sigma}{4(t - t')} \right] \\ \times I_1 \left[\frac{rr'\mu\sigma}{4(t - t')} \right] ,$$

where $I_1(x)$ is the Bessel function of the second kind and first order. Also, the k integral can be done using the result

$$\frac{1}{2\pi} \int dk \exp \left[-\frac{k^2(t - t')}{\mu\sigma} + ik(z - z' - D) \right] \\ = \left[\frac{\mu\sigma}{4\pi(t - t')} \right]^{1/2} \exp \left[-\frac{\mu\sigma}{4(t - t')} (z - z' - D)^2 \right] ,$$

where

$$D = \int_{t'}^t v_0(t'') dt'' .$$

Thus, the Green's function is

$$G(r, r', z, z', t, t') = -\frac{\theta(t - t')}{4(t - t')^{3/2}} \left(\frac{\mu\sigma}{\pi} \right)^{1/2} \\ \times \exp \left\{ -\frac{\mu\sigma}{4(t - t')} \left[(z - z' - D)^2 + (r - r')^2 \right] \right\} \\ \times \exp \left[-\frac{rr'\mu\sigma}{2(t - t')} \right] I_1 \left[\frac{rr'\mu\sigma}{2(t - t')} \right] . \quad (11)$$

EVALUATION OF VOLTAGE IN PICKUP COIL

The voltage V in the pickup coil is determined by the rate of change of the magnetic flux linking the coil. In terms of the vector potential A , the voltage is given by

$$V(t) = 2\pi R \frac{\partial}{\partial t} A(R, z_0, t) . \quad (12)$$

Using Eq. (6), this expression becomes

$$\begin{aligned} V(t) &= 2\pi R \frac{\partial}{\partial t} \iiint -\mu G(R, z_0, t, r', z', t') \\ &\quad \times J(r', z', t') dr' dz' dt' . \end{aligned}$$

It follows from Eqs. (3) and (11) that $V(t)$ is

$$\begin{aligned} V(t) &= 2\pi Ra\mu I \frac{\partial}{\partial t} \int dt' \frac{\theta(t - t')}{4(t - t')^{3/2}} \left(\frac{\mu\sigma}{\pi} \right)^{1/2} \\ &\quad \times \exp \left[-\frac{\mu\sigma}{4(t - t')} \left\{ [z - f(t') - D]^2 + (R - a)^2 \right\} \right] \\ &\quad \times \exp \left[-\frac{aR\mu\sigma}{2(t - t')} \right] I_1 \left[\frac{aR\mu\sigma}{2(t - t')} \right] . \end{aligned} \quad (13)$$

Taking the indicated derivatives and changing variables results in the final expression for the voltage:

$$\begin{aligned} V(t) &= \frac{\sqrt{\pi}}{4} Ra\mu I \int_0^\infty dx \sqrt{x} [z_0 - f(\gamma) - D][v(\gamma) + v_0(t) - v_0(\gamma)] \\ &\quad \times \exp \left[-\frac{x}{4} \left\{ [z_0 - f(\gamma) - D]^2 + (R - a)^2 \right\} \right] \exp \left(-\frac{aR}{2} x \right) I_1 \left(\frac{aR}{2} x \right) , \end{aligned} \quad (14)$$

where

$$\gamma = t - \frac{\mu\sigma}{x} ,$$

$$D = \frac{\mu\sigma}{x} \int_0^1 v_0 \left(t - \frac{\mu\sigma}{x} y \right) dy ,$$

and

$$v(t) = \frac{df(t)}{dt} .$$

SECTION 4
ANALYSIS OF MODEL 3

Model 3 encompasses models 1 and 2 but also includes the effects of the moving shock-induced conductivity front. In model 3, the field coil is located at position $z = f(t)$, as before, and the shock front at $z = g(t)$. The medium has conductivity σ and velocity $v_0(t)$ for positions behind the shock wave [$z < g(t)$]; the conductivity and velocity are zero for positions in front of the shock wave [$z > g(t)$]. We label as region 1 the shocked region, where $\sigma \neq 0$; and as region 2 the unshocked region, where $\sigma = 0$. The fields that exist before the interface (shock wave) has passed the field coil are labeled with a superscript b.

Before the interface reaches the field coil, the field in region 1 is a solution to

$$\left(\nabla^2 - \frac{1}{r^2} - \mu\sigma \frac{\partial}{\partial t} - \mu\sigma v_0 \frac{\partial}{\partial z} \right) A_1^b = 0 .$$

This solution can be represented as

$$A_1^b = -\mu I_0 \int dk_1 dk_2 J_1(k_1 r) \\ \times \exp \left[+ik_2 D - ik_2 z - \frac{(k_1^2 + k_2^2)t}{\mu\sigma} \right] \hat{a}_1^b(k_1, k_2) .$$

In region 2, before the interface reaches the field coil, the field is

$$A_2^b = A_0^b + a_2^b , \quad (15)$$

where A_0^b is the field produced by the field coil,

$$A_0^b = - \int \mu G^b J_r' dr' dz' , \quad (16)$$

and a_2^b is a solution of

$$\left(\nabla^2 - \frac{1}{r^2} \right) a_2^b = 0 .$$

This expression can be represented as

$$a_2^b = - \mu I_0 \int dk e^{-kz} J_1(kr) \hat{a}_2^b(k) .$$

The Green's function G^b is given by

$$G^b(r, r', z, z') = - \frac{1}{2} \int d\xi \exp(-\xi|z - z'|) J_1(\xi r) J_1(\xi r') . \quad (17)$$

The functions a_1^b and a_2^b are determined by requiring that A and $\partial A / \partial z$ be continuous at $z = g(t)$ --that is, across the shock front. Imposing those conditions yields the following equations for \hat{a}_1^b , \hat{a}_2^b :

$$\begin{aligned} & \int dk_2 \exp \left[+ ik_2 D - ik_2 g - \frac{(k_1^2 + k_2^2)t}{\mu \sigma} \right] \left(1 - \frac{ik_2}{k_1} \right) \hat{a}_1^b(k_1, k_2) \\ &= - a \exp[-k_1(f - g)] J_1(k_1 a) \end{aligned} \quad (18)$$

and

$$\begin{aligned} & \int dk_2 \exp \left[+ ik_2 D - ik_2 g - \frac{(k_1^2 + k_2^2)t}{\mu \sigma} \right] \left(1 + \frac{ik_2}{k_1} \right) \hat{a}_1^b(k_1, k_2) \\ &= 2 \exp(-k_1 g) \hat{a}_2^b(k_1) . \end{aligned} \quad (19)$$

Equation (18) can be solved for \hat{a}_1^b and then used in Eq. (19) to obtain \hat{a}_2^b .

After the interface has passed the field coil, a slightly different set of equations applies. Now the field in the conducting region includes that of the field coil so, in region 1, we have

$$A = A_0 + A_1 ,$$

where

$$A_0 = - \mu \int G J r' dr' dz' dt' ,$$

with G given by Eq. (11), and

$$A_1 = - \mu I_0 \int dk_1 dk_2 J_1(k_1 r) \\ \times \exp \left[+ ik_2 D - ik_2 z - \frac{(k_1^2 + k_2^2)t}{\mu \sigma} \right] \hat{a}_1(k_1, k_2) .$$

The field in region 2, after the interface has passed the field coil, is given by

$$a_2 = - \mu I_0 \int dk e^{-kz} J_1(kr) \hat{a}_2(k) . \quad (20)$$

The quantities \hat{a}_1 and \hat{a}_2 are determined, as before, by requiring A and $\partial A / \partial z$ to be continuous at $z = g(t)$. Imposing those conditions yields the following equations for \hat{a}_1 , \hat{a}_2 :

$$\begin{aligned}
& \int dk_2 \left(1 - \frac{ik_2}{k_1} \right) \exp \left[+ ik_2 D - ik_2 g - \frac{(k_1^2 + k_2^2)}{\mu\sigma} t \right] \hat{a}_1(k_1, k_2) \\
& - \int dt' k_1 J_1(k_1 a) \left[1 - \frac{\mu\sigma}{2(t - t')k_1} (g - f - D) \right] \left[\frac{a^2}{4\pi(t - t')\mu\sigma} \right]^{1/2} \\
& \times \exp \left[- \frac{k_1^2}{\mu\sigma} (t - t') - \frac{\mu\sigma}{4(t - t')} (g - f - D)^2 \right] = 0 \tag{21}
\end{aligned}$$

and

$$\begin{aligned}
& \int dk_2 \left(1 + \frac{ik_2}{k_1} \right) \exp \left[+ ik_2 D - ik_2 g - \frac{(k_1^2 + k_2^2)}{\mu\sigma} t \right] \hat{a}_1(k_1, k_2) \\
& - \int dt' k_1 J_1(k_1 a) \left[1 + \frac{\mu\sigma}{2(t - t')k_1} (g - f - D) \right] \left[\frac{a^2}{4\pi(t - t')\mu\sigma} \right]^{1/2} \\
& \times \exp \left[- \frac{k_1^2}{\mu\sigma} (t - t') - \frac{\mu\sigma}{4(t - t')} (g - f - D)^2 \right] = 2\hat{a}_2(k_1, t) e^{-k_1 g} \tag{22}
\end{aligned}$$

Equation (21) can be solved for $\hat{a}_1(k_1, k_2)$ and used in Eq. (22) to obtain $\hat{a}_2(k_1, t)$.

The voltage in the pickup coil is then obtained using Eqs. (12) and (15), (16), (17), or (20).

Numerical solution of Eqs. (18), (19), (21), and (22) is difficult because \hat{a}_1 is a sharply peaked function having a maximum at $k_1 \approx -ik_2$. Thus, an appropriate method of solution is used here. Equation (18) can be satisfied only if

$$-k_1 g - ik_2(g - D) - \frac{(k_1^2 + k_2^2)t}{\mu\sigma} = 0$$

or

$$\frac{ik_2}{k_1} = \frac{\mu\sigma(g - D)}{2tk_1} - \left\{ \left[1 + \frac{\mu\sigma(g - D)}{2tk_1} \right]^2 + \frac{\mu\sigma D}{k_1 t} \right\}^{1/2}.$$

For small values of σ , this expression is

$$\frac{ik_2}{k_1} \approx -1 - \frac{\mu\sigma D}{2k_1 t}.$$

For large values of σ , it is

$$\frac{ik_2}{k_1} \approx -\frac{g}{g - D}.$$

Assuming $a_1(k_1, k_2) \sim a_1 \delta(\tilde{k}_2 - k_1)$, then Eqs. (18) and (19) can be solved to yield

$$a_2 = -\frac{a^2 R \mu I}{32} \frac{\mu\sigma D}{t} \frac{1}{(z + f - 2g)^2} \quad (23a)$$

for σ small and

$$a_2 = -\frac{a^2 R \mu I D}{4(2g - D)} \frac{1}{(z + f - 2g)^3} \quad (23b)$$

for σ large. For our problem, σ is almost always small ($< 10^3$ mhos/m). Thus, using Eq. (23a), we evaluate the voltage in the pickup coil before the field coil starts to move (i.e., $g < f$) as

$$V = - \frac{\pi R^2 a^2}{16t} \frac{\mu\sigma}{(z_0 + f - 2g)^2} \mu I \left[v_0(t) - \frac{D(t)}{t} + \frac{4v_s(t)D(t)}{(z_0 + f - 2g)} \right]. \quad (24a)$$

Here $v_s(t)$ is the shock velocity, $v_s(t) = \partial g / \partial t$. For very large conductivities, the voltage is

$$V = - \frac{\pi R^2 a^2 \mu I}{2g - D} \frac{1}{(f + z - 2g)^3} \left[\frac{(gv_0 + Dv_s - Dv_0)}{2g - D} + \frac{3v_s D}{f + z_0 - 2g} \right]. \quad (24b)$$

For the case when the shock wave has passed the field coil, the contribution of \hat{a}_1 to Eq. (22) is negligible. Thus,

$$\begin{aligned} a_2 &= \frac{\mu I}{2} \left(\frac{a^2}{4\pi\mu\sigma} \right)^{1/2} \int dt' \int dk \\ &\times \exp \left[- \frac{k^2(t - t')}{\mu\sigma} + \frac{\mu\sigma}{4(t - t')} (g - f - D)^2 + k(z - g) \right] \\ &\times \frac{k J_1(ka) J_1(kr)}{\sqrt{t - t'}} \left[1 + \frac{\mu\sigma}{2(t - t')} \frac{(g - f - D)}{k} \right]. \end{aligned}$$

After the small-argument approximation for the Bessel functions has been used, one integration can be performed and the result put into a more convenient form:

$$\begin{aligned} a_2 &= \frac{a^2 R \mu I}{8(z - g)^3} \int dx e^{-\lambda^2 x} \left\{ \left[2 \left(\frac{x}{\pi} \right)^{1/2} \psi(2, 1/2, x) \right. \right. \\ &\left. \left. - 4 \left(\frac{x}{\pi} \right)^{1/2} \lambda x \psi(2, 3/2, x) \right] + \exp x \left[2x^2(\lambda - 1) + x(\lambda - 3) \right] \right\}, \quad (25) \end{aligned}$$

where $\psi(a, b, x)$ is the confluent hypergeometric function of the first kind (regular at $x = 0$) and λ is given by

$$\lambda = \frac{g(t) - f\left(t - \frac{\gamma}{x}\right) - d(t, x)}{z - g(t)},$$

with

$$\gamma = [z - g(t)]^2 \frac{\mu\sigma}{4}$$

and

$$d(t, x) = \int_0^{\gamma/x} v_0(t - y) dy.$$

Equation (25) can also be written as

$$a_2 = \frac{a^2 R \mu I}{8(z - g)^3} \int_0^\infty dx e^{-\lambda^2 x} \left(\frac{x}{\pi}\right)^{1/2} \left[\frac{3}{2} U(2, 1/2, x) + \lambda x U(2, 3/2, x) \right], \quad (26)$$

where $U(a, b, x)$ is the confluent hypergeometric function of the second kind (singular at $x = 0$). The voltage is obtained from the vector potential using Eq. (12):

$$v = \frac{\pi R^2 a^2 \mu I}{2 \sqrt{\pi} (z_0 - g)^3} \int dy y^2 \exp(-\lambda^2 y^2) \left\{ \left[\frac{3v_s}{(z_0 - g)} - 2\lambda \dot{y}^2 \right] \right. \\ \left. \times \left[\frac{3}{2} U(2, 1/2, y^2) + \lambda y^2 U(2, 3/2, y^2) \right] + \dot{y}^2 U(2, 3/2, y^2) \right\}, \quad (27)$$

where

$$\dot{\lambda} = \frac{v_s(\lambda + 1) - \left(1 - \frac{\dot{\gamma}}{y^2}\right) \left[v_0 \left(t - \frac{\gamma}{y^2}\right) - v \left(t - \frac{\gamma}{y^2}\right) \right] - v_0(t)}{z_0 - g}$$

with

$$\dot{\gamma} = - \frac{\mu \sigma v_s (z_0 - g)}{2} .$$

In the limit as $\sigma \rightarrow 0$, we have $d \rightarrow 0$, $\gamma \rightarrow 0$ and Eq. (27) reduces to

$$v = \frac{3\pi\mu I a^2 R^2}{2(z_0 - f)^4} v(t) .$$

SECTION 5
NUMERICAL RESULTS

To obtain numerical results, we evaluate the expressions in Eqs. (14), (24), and (26). The velocities were parameterized as zero for $t < 0$ and as

$$v_0(t) = \bar{v}_0 \left[\exp\left(-\frac{t}{\tau_1}\right) - \exp\left(-\frac{t}{\tau_2}\right) \right],$$

$$v(t) = \bar{v} \left\{ \exp\left[-\frac{(t - t_0)}{\tau_3}\right] - \exp\left[-\frac{(t - t_0)}{\tau_2}\right] \right\},$$

$$v_s(t) = \bar{v}_s \left[\exp\left(-\frac{t}{\tau_4}\right) - \exp\left(-\frac{t}{\tau_2}\right) \right]$$

for $t > 0$ and all velocities are zero for their arguments less than zero. The distances are taken as zero for $t < 0$ and as

$$D(t) = \bar{v}_0 \left\{ \left[1 - \exp\left(-\frac{t}{\tau_1}\right) \right] \tau_1 - \left[1 - \exp\left(-\frac{t}{\tau_2}\right) \right] \tau_2 \right\},$$

$$f(t) = f_0 + \bar{v} \left[\left\{ 1 - \exp\left[-\frac{(t - t_0)}{\tau_3}\right] \right\} \tau_3 - \left\{ 1 - \exp\left[-\frac{(t - t_0)}{\tau_2}\right] \right\} \tau_2 \right],$$

$$g(t) = \bar{v}_s \left\{ \left[1 - \exp\left(-\frac{t}{\tau_4}\right) \right] \tau_4 - \left[1 - \exp\left(-\frac{t}{\tau_2}\right) \right] \tau_2 \right\}$$

for $t > 0$.

We evaluated Eqs. (14), (24), and (26) using the following values for f_0 , z_0 , \bar{v} , \bar{v}_0 , \bar{v}_s , τ_1 through τ_4 , t_0 , and σ :

$$f_0 = g(t_0) = 0.25 \text{ m},$$

$$z_0 = 0.75 \text{ m},$$

$$\bar{v} = 10^3 \text{ m/sec},$$

$$\bar{v}_0 = \bar{v} \exp(t_0/\tau_1) = 1.63 \times 10^3 \text{ m/sec},$$

$$\bar{v}_s = 3 \times 10^3 \text{ m/sec},$$

$$\tau_1 = \tau_3 = 2 \times 10^{-4} \text{ sec},$$

$$\tau_2 = 10^{-5} \text{ sec},$$

$$\tau_4 = 10^{-3} \text{ sec},$$

$$t_0 = 9.8 \times 10^{-5} \text{ sec},$$

$$\sigma = 0, 10, 100 \text{ mhos/m.}$$

These parameter values are similar to those appropriate for MINI JADE and MISTY JADE. The results for these values are plotted for models 2 and 3 in Figs. 2 and 3, respectively.

Knowing the value of the shock-induced conductivity and using the theory developed above, it is possible to determine the particle velocity from the gauge response. However, the value of the shock-induced conductivity is rarely well known. Thus, the gauge should be used to measure particle velocity only in situations where the effect of the conductivity does not depend strongly on the value of the conductivity.

Figures 2 and 3 show that, for typical gauge parameter values, shock-induced conductivity just begins to affect the gauge response at 100 mhos/m. We thus conclude that, for measurements of MINI JADE and MISTY JADE phenomena, shock-induced conductivity has little effect on gauge response as long as it is less than 100 mhos/m.

Figure 3 shows the magnitude and time dependence of the precursor signal caused by the advancing conductivity front before the field coil begins to move. It has been suggested that the precursor signal could be

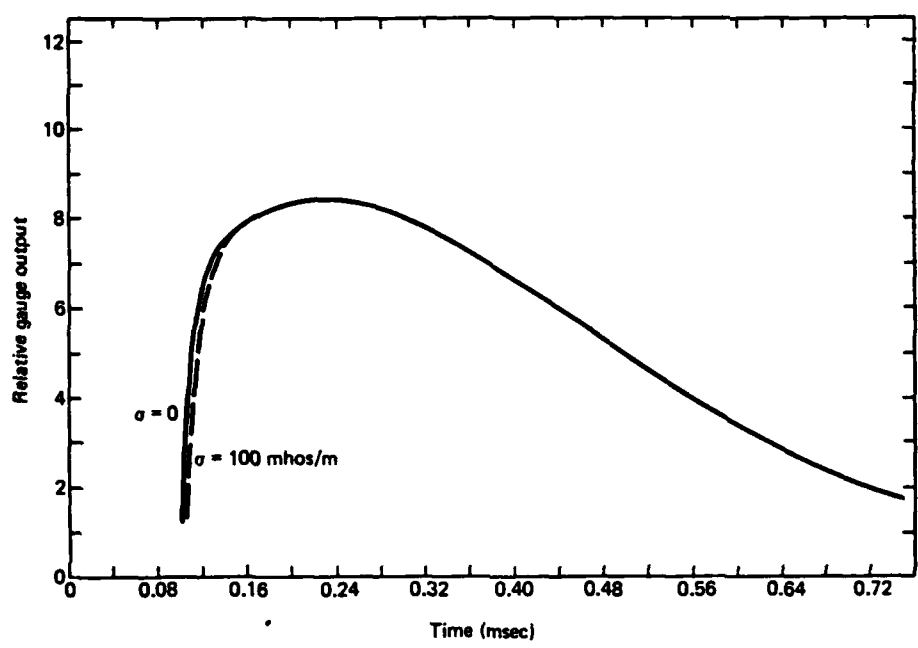


Figure 2. Gauge output versus time for model 2.

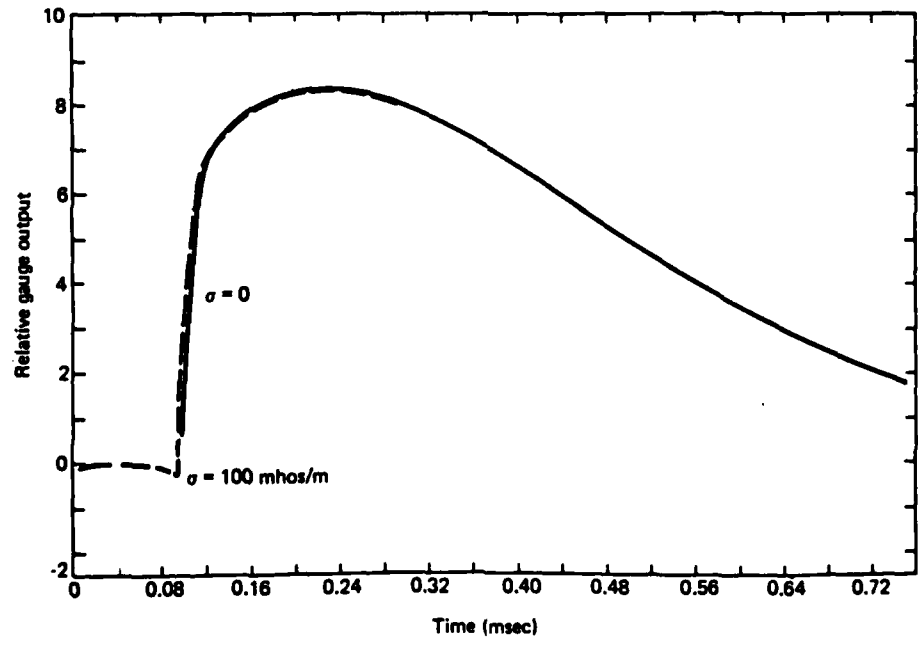


Figure 3. Gauge output versus time for model 3.

used to deduce the medium velocity before the field coil begins to move. However, Fig. 3 indicates that, when the gauge is designed to measure the signal from the moving field coil (and consequently $\sigma < 100$ mhos/m), the precursor signal is probably too small to be reliably used to measure the medium velocity.

If one is willing to design the gauge to measure *only* the precursor signal, then, according to Eqs. (24a) and (24b) for the gauge response, in certain ranges of conductivity, the gauge could measure either the shock-induced conductivity or the medium velocity. That is, Eq. (24a) shows that, for $\sigma < 1000$ mhos/m, the gauge response is linear in the conductivity, so precursor signal measurements along with independent measurements of the medium velocity and shock velocity could be used to determine the medium conductivity. Further, Eq. (24b) shows that, for $\sigma > 1000$ mhos/m, the precursor signal is once again independent of the shock-induced conductivity. Thus, for very large conductivities (> 1000 mhos/m), the precursor signal could be used to measure the medium velocity.

We conclude that the Kratz particle velocity gauge is not sensitive to shock-induced conductivity for conductivities less than about 100 mhos/m. For gauges designed to measure the velocity of the field coil, the precursor signal is probably too small to be useful. However, gauges can be designed to take advantage of the precursor signal and measure either the shock-induced conductivity (for $\sigma < 1000$ mhos/m) or the medium velocity (for $\sigma > 1000$ mhos/m).

REFERENCES

Coleman, P., briefing presented at the HURON LANDING review conducted at the Defense Nuclear Agency Field Command, Albuquerque, New Mexico, 1982.

-----, briefing presented at the MINI JADE review conducted at the Defense Nuclear Agency Field Command, Albuquerque, New Mexico, 1983.

Gradshteyn, I. S., and I. M. Ryzhik, *Table of Integrals, Series, and Products*, A. Jeffrey (ed.), Academic Press, New York, 1980.

Kratz, H. R., *HUSKY PUP Debris Impact Experiment--Development and Fielding of an Electromagnetic Particle Velocity Gauge, Systems, Science and Software*, La Jolla, California, SSS-R-76-2950, 1976.

Schlessinger, L., *Analysis of Particle Velocity Gauges for MISTY JADE*, Pacific-Sierra Research Corporation, Note 357, February 1981.

APPENDIX
LIST OF SYMBOLS

a = radius of field coil

a_2 = vector potential in region 2 (which has no shock-induced conductivity) after shock wave has passed field coil

a_2^b = contribution to vector potential in region 2 (which has no shock-induced conductivity) caused by presence of conductivity front before shock wave has passed field coil, i.e., $A_2^b = A_0^b + a_2^b$

$\hat{a}_1, \hat{a}_2, \hat{a}_1^b, \hat{a}_2^b$ = Bessel transforms of a_1, a_2, a_1^b, a_2^b

\vec{A} = vector potential

A_0 = vector potential of field coil in homogeneous moving medium with shock-induced conductivity

A_1 = contribution to vector potential in region 1 (which has shock-induced conductivity) caused by presence of conductivity front after shock wave has passed field coil

A_0^b = vector potential of field coil in homogeneous medium of zero conductivity

A_1^b = vector potential in region 1 (which has shock-induced conductivity) before shock wave has passed field coil

A_2^b = vector potential in region 2 (which has no shock-induced conductivity) before shock wave has passed field coil

b = superscript indicating fields that exist before shock wave has passed field coil

\vec{B} = magnetic field

D = time integral of medium velocity

\vec{E} = electric field

$f(t)$ = axial position of field coil

$g(t)$ = axial position of shock wave

G = Green's function

G^b = Green's function for field coil in medium of zero conductivity

I = current in field coil (assumed constant)

\vec{J} = current density

r = radial coordinate of cylindrical coordinate system

R = radius of pickup coil

$U(a, b, x)$ = confluent hypergeometric function of second kind
(singular at $x = 0$)

$v(t)$ = field coil velocity

$v_0(t)$ = medium velocity

v_s = axial velocity of shock wave

V = voltage in pickup coil

z = axial coordinate of cylindrical coordinate system

z_0 = axial position of pickup coil

$\delta(x)$ = Dirac delta function

ϕ = azimuthal angle of cylindrical coordinate system

Φ = scalar potential

$\psi(a, b, x)$ = confluent hypergeometric function of first kind (regular at $x = 0$)

σ = medium conductivity

μ = medium permeability (taken to be that of free space)

DISTRIBUTION LIST

DEPARTMENT OF DEFENSE

Asst to the Secy of Defense, Atomic Energy
ATTN: Executive Assistant

Defense Intelligence Agency
ATTN: RTS-2B

Defense Nuclear Agency
ATTN: SPTD
2 cy ATTN: SPSS
4 cy ATTN: STTI-CA

Defense Technical Information Center
12 cy ATTN: DD

Field Command, DNA, Det 2
Lawrence Livermore National Lab
ATTN: FC-1

Field Command, Defense Nuclear Agency
ATTN: FCPR
ATTN: FCT
ATTN: FCTT
ATTN: FCTT, W. Summa
ATTN: FCTXE

Under Secy of Def for Rsch & Engrg
ATTN: Strat & Space Sys (OS)

DEPARTMENT OF THE ARMY

Harry Diamond Laboratories
ATTN: DELHD-NW-P, 20240
ATTN: 00100, Commander/Tech Dir/Div Dir

US Army Ballistic Research Lab
ATTN: DRDAR-BLA-S, Tech Library
ATTN: DRDAR-BLT, J. Keefer

US Army Chemical School
ATTN: ATZN-CM-CS

US Army Cold Region Res Engr Lab
ATTN: CRREL-EM

US Army Engr Waterways Exper Station
ATTN: F. Hanes
ATTN: J. Ingram
ATTN: Library
ATTN: WESSE, D. Day

US Army Material Command
ATTN: DRXAM-TL, Tech Library

US Army Nuclear & Chemical Agency
ATTN: Library

US Army White Sands Missile Range
ATTN: STEWS-TE-N, K. Cummings

DEPARTMENT OF THE NAVY

David Taylor Naval Ship R&D Ctr
ATTN: Code 1770
ATTN: Tech Info Ctr, Code 522.1

Naval Surface Weapons Center
ATTN: Code F31

DEPARTMENT OF THE AIR FORCE

Air Force
ATTN: INT

Air Force Institute of Technology
ATTN: Library

Air Force Weapons Laboratory
ATTN: DEX
ATTN: NTE, M. Plamondon
ATTN: NTED, J. Renick
ATTN: SUL

Air University Library
ATTN: AUL-LSE

Ballistic Missile Office/DAA
ATTN: PP
2 cy ATTN: ENSM

DEPARTMENT OF ENERGY

Department of Energy
Albuquerque Operations Office
ATTN: CTID

Department of Energy
Nevada Operations Office
ATTN: Doc Con for Tech Library

OTHER GOVERNMENT AGENCIES

Central Intelligence Agency
ATTN: OSWR/NED

Department of Interior
US Geological Survey
ATTN: D. Roddy

Federal Emergency Management Agency
ATTN: Ofc of Rsch/NP, D. Bensen

NATO

NATO School, SHAPE
ATTN: US Documents Officer

DEPARTMENT OF ENERGY CONTRACTORS

University of California
Lawrence Livermore National Lab
ATTN: Tech Info Dept Library

Oak Ridge National Laboratory
ATTN: Civ Def Res Proj, Mr Kearny

Sandia National Laboratories
ATTN: Library & Security Classification Div

Sandia National Laboratories
ATTN: Div 7111, B. Vortman
ATTN: Tech Lib 3141

DEPARTMENT OF DEFENSE CONTRACTORS

Aurex Corp
ATTN: K. Triebes

DEPARTMENT OF DEFENSE CONTRACTORS (Continued)

Aerospace Corp
ATTN: Library Acquisition M1/199

Agbabian Associates
ATTN: M. Agbabian

Applied Research Associates, Inc
ATTN: D. Piepenburg

Applied Research Associates, Inc
ATTN: R. Frank

Artec Associates, Inc
ATTN: D. Baum

BDM Corp
ATTN: Corporate Library
ATTN: T. Neighbors

Boeing Co
ATTN: Aerospace Library

California Research & Technology, Inc
ATTN: K. Kreyenhagen

California Research & Technology, Inc
ATTN: F. Sauer

Cushing Associates
ATTN: V. Cushing

Develco, Inc
ATTN: L. Rorden

EG&G Wash Analytical Svcs Ctr, Inc
ATTN: Library

Electro-Mech Systems, Inc
ATTN: H. Piper
ATTN: R. Shunk

General Research Corp
ATTN: E. Steele
ATTN: R. Parisse

Geo Centers, Inc
ATTN: H. Linnerud
ATTN: L. Isaacson

H-Tech Labs, Inc
ATTN: B. Hartenbaum

Horizons Technology, Inc
ATTN: R. Kruger

IIT Research Institute
ATTN: Documents Library

Kaman Sciences Corp
ATTN: Library

Kaman Tempo
ATTN: DASIAC
ATTN: J. Shoutens

Kaman Tempo
ATTN: DASIAC

DEPARTMENT OF DEFENSE CONTRACTORS (Continued)

Merritt CASES, Inc
ATTN: J. Merritt
ATTN: Library

Mitre Corp
ATTN: J. Freedman

University of New Mexico
ATTN: N. Baum

Pacific-Sierra Research Corp
ATTN: H. Brode, Chairman SAGE
2 cy ATTN: L. Schlessinger

Physics Applications, Inc
ATTN: C. Vincent

- R&D Associates
ATTN: P. Haas
ATTN: Tech Info Center
ATTN: J. Lewis

R&D Associates
ATTN: G. Ganong

Rand Corp
ATTN: P. Davis

Rand Corp
ATTN: B. Bennett

S-CUBED
ATTN: D. Grine
ATTN: Library

Science & Engrg Associates, Inc
ATTN: B. Chambers III
ATTN: J. Stockton

Science Applications Intl Corp
ATTN: K. Sites

Science Applications Intl Corp
ATTN: Tech Library

Science Applications Intl Corp
ATTN: W. Layson

Southwest Research Institute
ATTN: A. Wenzel
ATTN: W. Baker

SRI International
ATTN: D. Keough
ATTN: G. Abrahamson
ATTN: P. De Carli

Structural Mechanics Associates, Inc
ATTN: R. Kennedy

Teledyne Brown Engineering
ATTN: D. Ormond
ATTN: F. Leopard

Terra Tek, Inc
ATTN: S. Green

DEPARTMENT OF DEFENSE CONTRACTORS (Continued)

TRW Electronics & Defense Sector
ATTN: Tech Info Center
2 cy ATTN: N. Lipner

TRW Electronics & Defense Sector
ATTN: E. Wong
ATTN: P. Dai

DEPARTMENT OF DEFENSE CONTRACTORS (Continued)

Weidlinger Assoc. Consulting Engrg
ATTN: T. Deevy

Weidlinger Assoc. Consulting Engrg
ATTN: M. Baron

Weidlinger Assoc. Consulting Engrg
ATTN: J. Isenberg

END

FILMED

2-86

DTIC